

# QUANTITATIVE EVALUATION OF THE MICROSTRUCTURE IN AN FE-CR-C TERNARY MARTENSITIC STEEL WITH THE AID OF THE SYSTEM FREE ENERGY CONCEPT

Tomonori Kunieda - Graduate student, Nagoya University  
Yoshinori Murata - Department of Materials, Physics and Energy Engineering,  
Graduate School of Engineering, Nagoya University, Japan  
Toshiyuki Koyama - National Institute for Materials Science, Japan  
Masahiko Morinaga - Department of Materials, Physics and Energy Engineering,  
Graduate School of Engineering, Nagoya University, Japan  
Masaaki Nakai - Graduate student, Nagoya University

## ABSTRACT

Quantitative evaluation of the microstructure of an Fe-Cr-C ternary steel was performed using the system free energy concept. The system free energy ( $G_{\text{sys}}$ ) of the martensite structure in steels is defined as,  $G_{\text{sys}} = G_0 + E_{\text{surf}} + E_{\text{dis}}$ . Here,  $G_0$  is the chemical free energy,  $E_{\text{surf}}$  is the interfacial energy based on the boundaries associated with the martensite microstructure and  $E_{\text{str}}$  is the elastic strain energy based on the dislocation density in the martensite phase. From the experimental results on SEM/EBSD, the interfacial energies were evaluated to be 0.05J/mol for the prior austenite boundary of as-quench specimen, 0.11J/mol for the martensite packet boundary and 0.33J/mol for the martensite block and lath boundaries. Thus, the total interfacial energy was 0.47J/mol in the as-quenched state, and it decreased to about 0.28J/mol after annealing at 873K for 100h. On the other hand, the elastic strain energy of as-quenched specimen was evaluated to be 7.1J/mol. The total system free energy of martensite phase was about 7.6J/mol, which became a driving force for the following microstructure evolution.

## KEYWORDS

martensite phase, heat resistant steel, dislocation density, interfacial energy, elastic strain energy, system free energy, microstructure evolution

## INTRODUCTION

Microstructures of high Cr heat resistant steels are composed of the martensite phase,  $M_{23}C_6$  carbide, MX carbonitrides and intermetallic compounds (e.g., the Laves phase) as well as the ferritic phase [1, 2]. The creep strength of these steels was affected by the structural recovery of the martensite phase and the coalescence of both the Laves phase and the  $M_{23}C_6$  carbide. Recently, it has been reported that their long-term creep strength at 923K is much smaller than the value extrapolated from a short-term creep strength. Such a large decrease in the long-term creep strength is interpreted as due to the inhomogeneous microstructure evolution during creep [3]. Therefore, the quantitative evaluation of the microstructure change is importance for the understanding of the long-term creep strength for their steels. Thus, one of the subjects of important in these days is in how to quantify the microstructures of the steels.

Recently, we have proposed that the system free energy concept is useful for the quantitative estimation of the microstructure evolution in the steels [4]. This concept was made on the basis of the total energy change attendant on the microstructural change [5]. The purpose of this study is to evaluate the system free energy change in the course of the microstructure evolution of the martensite phase in a high Cr heat resistant ferritic steel [4].

## 1. THEORY OF THE SYSTEM FREE ENERGY

### 1.1 SYSTEM FREE ENERGY OF THE MARTENSITE PHASE

The system free energy is defined by the sum of a chemical free energy,  $G_0$ , an interfacial energy,  $E_{\text{surf}}$ , and an elastic strain energy,  $E_{\text{str}}$  [4]. Then, the system free energy of the martensite phase is expressed by the following equation,

$$G_{\text{sys}} = G_0 + E_{\text{surf}} + E_{\text{str}}. \quad (1)$$

Here, the chemical free energy,  $G_0$ , was set to be zero, because only the  $\alpha$ -phase was treated in this study and the  $G_0$  of the  $\alpha$ -phase was employed as a standard of  $G_{\text{sys}}$ , i.e. zero.  $E_{\text{surf}}$  was estimated by the area fraction obtained from the experimental results as explained later.  $E_{\text{str}}$  was calculated from the dislocation density in the martensite lath. The low carbon martensite such as the experimental steel is the lath martensite which contains dislocations but no twins, so that the elastic strain energy caused by the martensite transformation was assumed to be stored as the dislocation strain energy in the lath martensite. In such a case, the microstructure evolution from the martensite phase to the  $\alpha$ -phase proceeds by the driving force of  $E_{\text{surf}}+E_{\text{str}}$  ( $=G_{\text{sys}}-G_0$ ). Therefore it is expected that the estimation of  $G_{\text{surf}}+E_{\text{str}}$  makes it possible to predict the microstructure evolution.

### 1.2 INTERFACIAL ENERGY FOR THE MARTENSITE PHASE

The interfacial energy  $E_{\text{surf}}$  was evaluated using the following equation,

$$E_{\text{surf}} = A \cdot \varepsilon_i \cdot V_f, \quad (2)$$

where  $A$  is the interfacial area per unit volume,  $\varepsilon_i$  is energy density for the boundaries,  $i$  is the type of boundaries and  $V_f$  is the molar volume. The martensitic steels consist of the multi boundaries, i.e., the prior  $\gamma$  phase boundary and the martensite packet-, block- and lath-boundaries. Then, Eq.(2) is modified to the following equation,

$$E_{\text{surf}} = (A_b \varepsilon_b + A_p \varepsilon_p + A_a \varepsilon_a) \times V_f. \quad (3)$$

Here, the subscripts, a, p, and b, indicate the prior austenite grain boundary, the martensite packet boundary and the block boundaries, respectively. Both the lath and block boundaries are regarded as small-angle boundaries or twin boundaries, and sometimes these two boundaries are hard to be distinguished with each other. In Eq.(3), the  $\varepsilon_b$ ,  $\varepsilon_p$  and  $\varepsilon_a$  are set to be  $0.10\text{J/m}^2$ ,  $0.468\text{J/m}^2$ , and  $0.76\text{J/m}^2$ , respectively, in this study [5, 6].

### 1.3 ELASTIC STRAIN ENERGY FOR THE MARTENSITE PHASE

As will be mentioned in section 1.1, it was assumed that the elastic strain energy of the martensite phase could be equivalent to the dislocation strain energy. Then, the elastic strain energy is expressed by the following equation [7],

$$E_{\text{dis}} \approx \frac{\mu b^2}{4\pi} \ln \frac{R_e}{r} \times \rho, \quad (4)$$

where,  $\mu$  is the shear modulus and the value,  $\mu=8.0\times 10^{10}\text{N/m}^2$ , for pure iron was used in this study [8].  $b$  is magnitude of the Burgers vector, i.e.  $b=0.284\text{nm}$  for iron, and  $r$  is the radius of dislocation core to be set at  $5b$  in this study [7].  $R_e$  is the outer cut off radius for calculating the strain energy around a dislocation, and  $\rho$  is the dislocation density. Both  $R_e$  and  $\rho$  can be determined using experimental data.

## 2. EXPERIMENTAL PROCEDURE

### 2.1 STEEL PREPARATION

Fe-11Cr-0.1C (mass%) ternary steel was used in this study. The analyzed result of the chemical composition is listed in Table 1. The ingot of this steel was prepared by vacuum induction melting and processed by hot-forging in a conventional way. In order to control the grain size to be about  $100\mu\text{m}$ , this steel was normalized at  $1373\text{K}$  for 5h, followed by the tempering at  $993\text{K}$  for 20h. Subsequently, it was cut into a plate with the size of  $5\times 5\times 10\text{mm}$ . The plate was austenitized at  $1323\text{K}$  for 5h followed by quenching into water and then into liquid nitrogen. After this quenching treatment, the plate was annealed at  $873\text{K}$  for various times from 2h to 1000h. Also, a steel annealed at  $923\text{K}$  for 1 year was prepared as a full-annealed specimen in order to use as a reference, i.e., the non-strain ferrite phase.

Table 1 Chemical composition of steel investigated in this study, (mass%)

C	Cr	Fe
0.10	11.01	Bal.

N: 11 ppm as an impurity

### 2.2 MICROSTRUCTURE OBSERVATION

The specimen was polished mechanically with emery papers down to #2000 followed by the buff polishing with  $\text{Al}_2\text{O}_3$  powders down to  $0.3\mu\text{m}$ . In order to observe the prior austenite grain boundary, it was etched in a Vilella's reagent with a 50mol%-glycerin, 17mol%-nitric acid and 33mol%-hydrochloric acid. After the etching, the microstructure in the specimen was observed with an optical microscope (OM), a scanning electron microscope (SEM) equipped with an instrument for taking electron backscattered diffraction pattern (EBSD).

### 2.3 X-RAY DIFFRACTION PEAK PROFILE ANALYSIS

Dislocation density of each specimen was measured by the X-ray diffraction, using a modified Williamson-Hall plot as well as a modified Warren-Averbach plot [9-13]. The procedure is as follows; (i) Peak profiles of 110, 200, 211, 220, 310 and 222 reflections were measured with the Cu target operated at 40kV and 30mA. (ii) Integrated intensities of each reflections were normalized by the following equation,

$$\int_{-\infty}^{+\infty} I(S) dS = 1, \quad (5)$$

where  $I(S)$  is X-ray intensity [9]. Then the profiles were fitted by the pseudo-Voigt function [14].

The normalized profiles were expanded into the Fourier series which gave the real part of the Fourier coefficients,  $A(L)$  for each peak. (iii) The full-width at half-maximum (FWHM) of the normalized peaks can be evaluated by the modified Williamson-Hall plot,

$$\Delta K \cong \frac{0.9}{D} + \frac{\pi M^2 b^2}{2} \rho^{1/2} K \bar{C}^{1/2} + O(K^2 \bar{C}), \quad (6)$$

where  $K = 2 \sin \theta / \lambda$ , and  $\Delta K = 2 \cos \theta (\Delta \theta) / \lambda$  is the magnitude of FWHM.  $\theta$  is the diffraction angle and  $\lambda$  is X-ray wavelength.  $D$ ,  $\rho$  and  $b$  are the average particle size, the average dislocation density and the Burgers vector, respectively. Both  $M$  and  $O$  are the constants depending on the effective outer cut-off radius ( $R_e$ ) of dislocations.  $\bar{C}$  is the contrast factor of dislocations. The average dislocation contrast factors,  $\bar{C}_{hkl}$  for the specific  $hkl$  reflection can be represented as,

$$\bar{C} = \bar{C}_{h00} (1 - qH^2), \quad (7)$$

where  $\bar{C}_{h00}$  is the average dislocation contrast factor for  $h00$  reflections, and  $H^2$  is expressed as  $H^2 = (h^2 k^2 + h^2 l^2 + k^2 l^2) / (h^2 + k^2 + l^2)$ .  $q$  is a parameter depending on the elastic constants of the crystal and the character of the dislocations in the crystals. The value of  $C_{h00}$  is determined from the theoretical calculation [9], and  $C_{h00} = 0.285$  for pure iron was used in the present analysis. (iv) The parameter,  $q$ , depending on both the elastic constants of the crystal and the character of dislocations in the crystal was estimated by the following Eq.(8), which was obtained by the quadratic form of Eq.(6) and using Eq.(7).

$$\left[ (\Delta K)^2 - \alpha \right] / K^2 \cong \pi M^2 b^2 \sigma \bar{C}_{h00} (1 - qH^2) / 2. \quad (8)$$

Here,  $\alpha$  is equal to  $(0.9/D)^2$ , and the value of  $\alpha$  was set so as to obtain a linear relationship between the left side of Eq.(8) and  $H^2$ . As a result, the parameter  $q$  can be determined experimentally. (v) Now,  $\bar{C}$  is known and the dislocation density can be obtained by the modified Warren-Averbach method,

$$\ln A(L) \cong \ln A^s(L) - \rho B L^2 \ln \left( \frac{R_e}{L} \right) (K^2 \bar{C}) + Q (K^4 \bar{C}^2), \quad (9)$$

where  $A(L)$  is the real part of the Fourier coefficients,  $A^s$  is the size Fourier coefficient as defined by Warren,  $B = \pi b^2 / 2$ ,  $R_e$  is the effective outer cut-off radius of dislocations [13], and  $Q$  stands for the second-order terms of  $K^2 \bar{C}$  i.e.,  $K^4 \bar{C}^2$ .  $L$  is the Fourier length [9]. The dislocation density can be obtained from the coefficient of the second term in Eq.(9).

### 3. EXPERIMENTAL RESULTS

#### 3.1 MICROSTRUCTURE OBSERVATION

It was confirmed through the optical microscopic observation that the as-quenched steel exhibited only the martensite single phase without any retained austenite phase. Figure 1 shows the typical OM and SEM images taken from the ternary steel annealed at 873K for 2h and 100h. The

precipitates observed in SEM images in Fig.1 were identified as  $M_{23}C_6$  carbide by the X-ray diffraction experiment using the extracted residues. In order to obtain the area fraction of each boundary, the average sizes of the prior  $\gamma$  grain, martensite packets and blocks were measured by an image analyzing method using their OM and SEM images. The average grain size was about  $150\mu\text{m}$  for prior  $\gamma$  grain,  $32\mu\text{m}$  for martensite packet,  $1\mu\text{m}$  for martensite block with annealing for 2h. The interfacial energy of each interface in unit volume was calculated by Eq.(2) using the measured grain sizes, and the result is shown in Fig.2. It was found that the martensite block exhibited the largest interfacial energy among the interfaces, but the value was only about  $0.2\text{J/mol}$  after annealing for 2h. On the other hand, the prior  $\gamma$  grain showed the smallest interfacial energy of about  $0.05\text{J/mol}$  after annealing for 2h. This difference is attributed mainly to the difference in the area fraction.

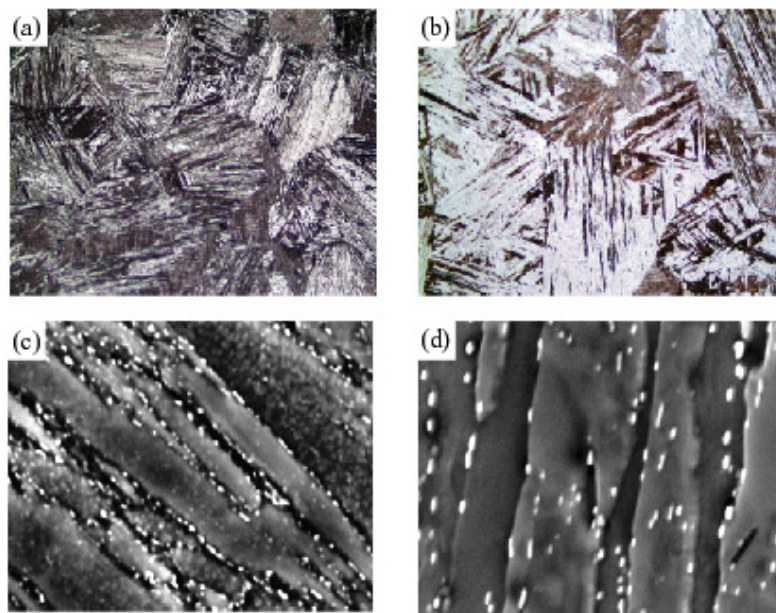


Fig.1 OM microstructure, (a) and (b) and SEM microstructure, (c) and (d) of the ternary steel. (a) and (c) are taken from the specimens annealed at 873K for 2h, and (b) and (d) are taken from the specimens annealed at 873K for 1000h.

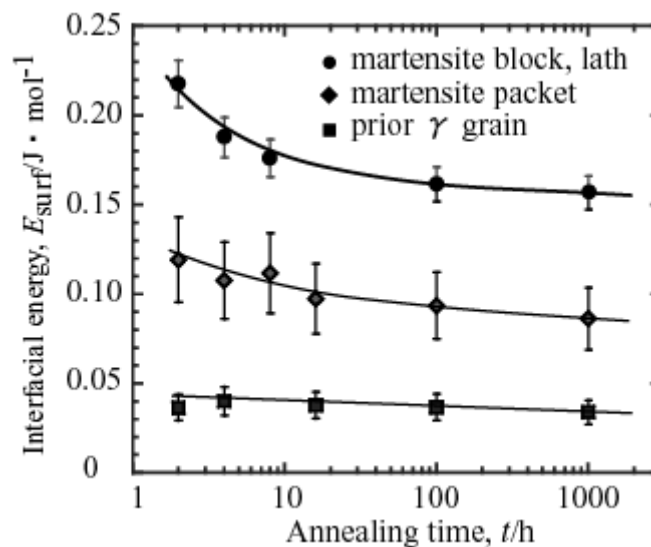


Fig.2 Changes in the interfacial energies of the prior  $\gamma$  grain, martensite packet, martensite block and lath with annealing time at 873K.

As shown in Fig.3, the total interfacial energy decreased quickly in the initial stage of annealing, but slowly in the later stage. The decrement was about 0.15J/mol. Here,  $E_{\text{surf}}$  of the as-quenched specimen could not be measured directly because of too fine microstructure. However, it can be estimated roughly to be 0.5J/mol using the data shown Fig.3.

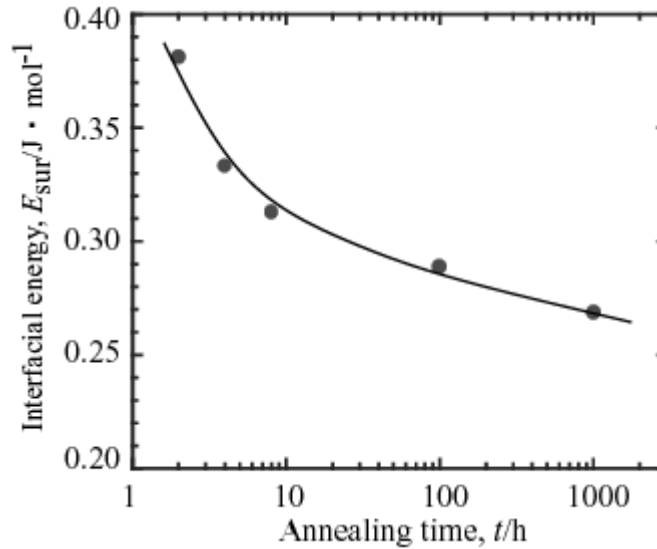


Fig.3 Change in the total interfacial energy with annealing time at 873K.

### 3.2 EVALUATION OF THE ELASTIC STRAIN ENERGY

Change in the elastic strain energy obtained from the modified Williamson-Hall plot and modified Warren-Averbach plot with annealing time is shown in Fig.4. The elastic strain energy of the as-quenched steel was about 7.1J/mol, and it decreased drastically in the initial stage of annealing. This value of the elastic strain energy is about twelve times higher than the total interfacial energy, and hence it is considered that the initial microstructure evolution occur by the driving force originated from the stress release. But the change became quite slow after 4h annealing, although the value did not reach the equilibrium one, i.e. about 0.30J/mol of the full-annealed  $\alpha$ -phase.

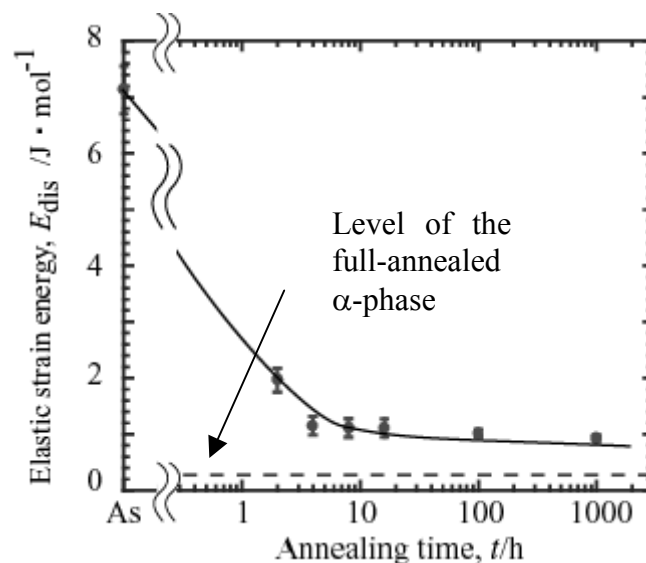


Fig.4 The change in the elastic strain energy with annealing at 873K

## 4. DISCUSSION

As mentioned above, the elastic strain energy ( $E_{\text{str}}$ ) of the as-quenched steel was about 7.1J/mol, whereas the interfacial energy ( $E_{\text{surf}}$ ) was about 0.5J/mol. Thus the elastic strain energy was larger by an order of magnitude than the interfacial energy in the as-quenched steel. In other words, most of the system free energy was the elastic strain energy in the as-quenched ternary steel.

The elastic strain energy, interfacial energy and total system free energy annealing at 873K was compared, as shown in Fig.5. Although the elastic strain energy accounts for the major part of the system free energy in the as-quenched state, it decreased abruptly to about 1.1J/mol with annealing at 873K for a few hours, and then decreased very slowly during the subsequent annealing. As a result, although the ratio of the interfacial energy to the total system free energy was very small in the as-quenched state, it increased and became about twenty percent after annealing at 873K for 100h. This result indicates that the role of the interfacial energy on the microstructure evolution becomes large in the later stage of annealing. In other words, it is considered that the strength of the martensite phase in the high Cr steels is subject to both the interfacial energy and the elastic strain energy in the later stage of creep.

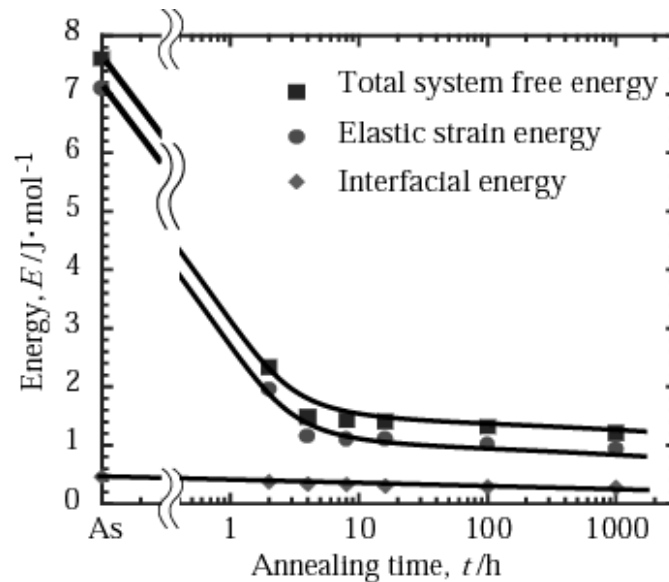


Fig.5 Changes in the total system energy, interfacial energy and elastic strain energy with annealing at 873K

When the standard energy level of the system free energy was set at that of the  $\alpha$ -phase, the system free energy in the full-annealed Fe-Cr-C steel was about 0.30J/mol. On the other hand, the system free energy after 1000h annealing at 873K was about 1.15J/mol as shown in Fig.5. Thus, the total free energy decreased very slowly during the subsequent annealing. Therefore, inhomogeneous nucleation of the ferrite phase might be necessary so as to approach the equilibrium value (the full-annealing state) for a finite annealing time. This is probably the reason why the inhomogeneous microstructure evolution is observed frequently in high Cr ferritic steels after a long-term creep test. In other words, the microstructure can reach at the equilibrium state easily by the inhomogeneous nucleation of the ferrite phase in martensite phase.

## 5. CONCLUSION

The system free energy of the martensite phase in an Fe-Cr-C ternary steel was estimated quantitatively. The total system free energy of the martensite phase was about 7.6J/mol in the as-quenched state when

the full-annealed  $\alpha$ -phase was selected as the standard energy level. When the as-quenched specimen was annealed at 873K for a few hours, the elastic strain energy decreased drastically from 7.1J/mol to about 1J/mol, and then kept decreasing very slowly during the subsequent annealing. It was found that the driving force for the microstructure evolution in the Fe-Cr-C martensitic steel arisen from the elastic strain energy in the initial stage of annealing but from both the interfacial energy and the elastic strain energy in the late stage of annealing.

## 6. ACKNOWLEDGEMENTS

The authors would like to thank The Japan Steel Works Ltd., for providing us the experimental steels. Also, we are grateful to Mr. M.Sugamuma in the Aichi Industrial Technology Institute for his kind support to use the X-ray diffractometry and his useful discussion for the analysis. This work was supported in part by the Grant-in-Aid for Scientific Research of the Japan Society for the Promotion of Science (JSJP), and also by “Nanotechnology Support Project of the Ministry of Education, Culture, Sports, Science and Technology (MEXT), Japan” in the Research Center for Ultrahigh Voltage Electron Microscopy, Osaka University.

## REFERENCES

- 1) T. FUJITA: ISIJ Int., 32 (1992), p175-181.
- 2) Y. MURATA, M. MORINAGA, R. HASHIZUME, K. TAKAMI, T. AZUMA, Y. TANAKA and T. ISHIGURO: Mater. Sci. Eng., A136 (2000), p251-261.
- 3) H. KUSHIMA, K. KIMURA and F. ABE: *Tetu-to-Hagane*, 85 (1999), p841-847.
- 4) Y. MURATA, T. KOYAMA, M. MORINAGA and T. MIYAZAKI: ISIJ Int., 42 (2002) p1423-1429.
- 5) T. MIYAZAKI and T. KOYAMA: Mater. Sci. Eng., A136 (1991), p151-159.
- 6) Y. ONO, K. KIMURA and T. WATANABE: Computer Assisted Microstructure Control of Steels, (2000) 99-108.
- 7) H. SUZUKI: *Teni-ron Nyumon*, (Agni, Japhan, 1967), p70.
- 8) *Kinzoku data book*, (The Japan Institute of Metals, 1984), p.35.
- 9) M. WILKENS: Phys. Stat. Sol. 2 (1970), p359-370.
- 10) T. UNGAR, I. DRAGOMIR, A. REVESZ and A. BORBELY: J. Appl. Cryst., 32 (1999), p992-1002.
- 11) F. YIN, T. HANAMURA, O. UMEZAWA and K. NAGAI: Mater. Sci. Eng., A354 (2003), p31-39.
- 12) T. UNGER, J. GUBICZA, G. RIBARIK and A. BORBELY: J. Appl. Cry., 34 (2001), p298-310.
- 13) T. UNGER and G. TICHY: Phys. Stat. Sol., 171 (1999), p425-434.
- 14) P. DAGUPTA: FIZIKA A (Zagreb), 9 (2000) 2, p61-66.